JOURNAL OF GEOPHYSICAL RESEARCH: OCEANS, VOL. 118, 5412–5425, doi:10.1002/jgrc.20322, 2013

Methanol, acetaldehyde, and acetone in the surface waters of the Atlantic Ocean

Rachael Beale,[1] Joanna L. Dixon,[1] Steve R. Arnold,[2] Peter S. Liss,[3,4] and Philip D. Nightingale[1]

Received 13 March 2013; revised 12 June 2013; accepted 16 July 2013; published 16 October 2013.

[1] Oceanic methanol, acetaldehyde, and acetone concentrations were measured during an Atlantic Meridional Transect (AMT) cruise from the UK to Chile (49°N to 39°S) in 2009. Methanol (48–361 n*M*) and acetone (2–24 n*M*) varied over the track with enrichment in the oligotrophic Northern Atlantic Gyre. Acetaldehyde showed less variability (3–9 n*M*) over the full extent of the transect. These oxygenated volatile organic compounds (OVOCs) were also measured subsurface, with methanol and acetaldehyde mostly showing homogeneity throughout the water column. Acetone displayed a reduction below the mixed layer. OVOC concentrations did not consistently correlate with primary production or chlorophyll-a levels in the surface Atlantic Ocean. However, we did find a novel and significant negative relationship between acetone concentration and bacterial leucine incorporation, suggesting that acetone might be removed by marine bacteria as a source of carbon. Microbial turnover of both acetone and acetaldehyde was confirmed. Modeled atmospheric data are used to estimate the likely air-side OVOC concentrations. The direction and magnitude of air-sea fluxes vary for all three OVOCs depending on location. We present evidence that the ocean may exhibit regions of acetaldehyde under-saturation. Extrapolation suggests that the Atlantic Ocean represents an overall source of these OVOCs to the atmosphere at 3, 3, and 1 Tg yr^{-1} for methanol, acetaldehyde, and acetone, respectively.

Citation: Beale, R., J. L. Dixon, S. R. Arnold, P. S. Liss, and P. D. Nightingale (2013), Methanol, acetaldehyde, and acetone in the surface waters of the Atlantic Ocean, *J. Geophys. Res. Oceans. 118*, 5412–5425, doi: 10.1002/jgrc.20322.

1. Introduction

[2] It is well documented that oxygenated volatile organic compounds (OVOCs) are ubiquitous throughout the atmosphere, where they influence the tropospheric ozone budget via photochemical decomposition [*Singh et al*., 1995, 2004; *Jacob et al*., 2005]. Oxidation and photochemical degradation of these species consumes hydroxyl (OH) radicals and can also create hydrogen oxide radicals (HO_x) and stable trace gases, altering the oxidative capacity of the troposphere [*Atkinson*, 2000; *Tie et al*., 2003; *Rosado-Reyes and Francisco*, 2007]. The role of the ocean is a major uncertainty in the global source inventories of OVOCs.

[3] Methanol is the most dominant OVOC and is second only to methane in relative abundance of organic gas in the atmosphere [*Heikes et al*., 2002]. The largest source of methanol to the troposphere is released from terrestrial biogenic material. Atmospheric oxidation by the OH radical is the major removal process [*Jacob et al*., 2005], which represents a significant source of both carbon monoxide and formaldehyde [*Millet et al*., 2008]. Acetone and acetaldehyde are both recognized precursors to the formation of the NO_x-sequestering stable trace gas, peroxyacetyl nitrate (PAN). Direct biogenic emissions and the oxidation of hydrocarbons are dominant sources of acetaldehyde and acetone to the atmosphere [*Singh et al*., 2004; *Jacob et al*., 2005; *Millet et al*., 2010]. The ocean is thought to release significant quantities of acetaldehyde, with the photodegradation of dissolved organic matter (DOM) the most likely in situ source [*Zhou and Mopper*, 1997]. Both of these carbonyl compounds undergo atmospheric oxidation [*Millet et al*., 2010], and acetone is also destroyed via photolysis [*Singh et al*., 1995; *Arnold et al*., 1997], which is its dominant sink in the dry upper troposphere [*Blitz et al*., 2004; *Arnold et al*., 2005].

[4] Evidence to establish the role of the ocean as a source or sink for these compounds is sparse due to a paucity of oceanic measurements. As a consequence, the processes driving the production and consumption of oceanic OVOCs remain unconstrained. Current direct seawater measurements of methanol, acetone, and acetaldehyde are limited to very specific regions of the North Atlantic [*Williams et al*., 2004; *Beale et al*., 2011; *Dixon et al*., 2011a,

[1]Plymouth Marine Laboratory, Plymouth, Devon, UK.
[2]Institute for Climate and Atmospheric Science, School of Earth and Environment, University of Leeds, Leeds, UK.
[3]School of Environmental Sciences, University of East Anglia, Norwich, UK.
[4]Department of Oceanography, Texas A&M University, College Station, Texas, USA.

Corresponding author: R. Beale, Plymouth Marine Laboratory, Plymouth, Devon PL1 3DH, UK. (rbea@pml.ac.uk)

2169-9275/13/10.1002/jgrc.20322

2011b], the North and Equatorial Pacific [*Marandino et al*., 2005; *Kameyama et al*., 2010], the Bahamas [*Zhou and Mopper*, 1997], and the Black Sea [*Mopper and Kieber*, 1991]. *Williams et al*. [2004] published methanol and acetone depth profiles noting higher surface concentrations than those observed at depth (150–200 m), and acetaldehyde below the mixed layer (as deep as 2 km) has previously been reported by *Mopper and Kieber* [1991].

[5] The dataset presented here represents the most comprehensive basin-wide spatial coverage of OVOC surface measurements in the Atlantic Ocean to date. We also present vertical profiles of methanol, acetaldehyde, and acetone concentrations along our transect of the Atlantic Ocean. These data allow investigation into potential relationships between OVOC concentrations and other biogeochemical variables (e.g., primary production, bacterial production, and chlorophyll-a), which, if significant, could enhance the ability to accurately model oceanic and atmospheric OVOC budgets. In addition, source and sink mechanisms which may be influencing OVOC concentrations throughout the Atlantic Ocean are discussed. Furthermore, a global model of atmospheric chemistry has been applied, optimized to best capture observed OVOC abundances in the tropical Atlantic atmospheric boundary layer [*Read et al*., 2012], to specify the atmospheric OVOC concentrations likely to have been present in the marine boundary layer at the time of water sampling. This allows estimation of both the direction and the strength of OVOC fluxes.

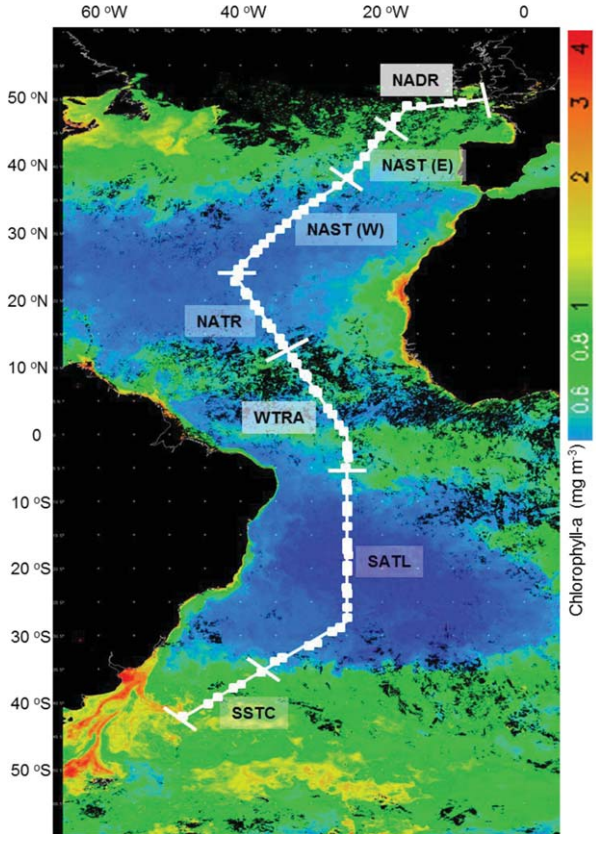

Figure 1. Composite chlorophyll-a image of the Atlantic Ocean over the period of October to December 2009 (supplied by NEODAAS) with superimposed cruise track through Atlantic provinces (defined by *Longhurst* [1995] in combination with fluorescence data). Where NADR; North Atlantic Drift Region, NAST(E); North Atlantic SubTropical gyre (East), NAST(W); North Atlantic SubTropical gyre (West), NATR; North Atlantic Tropical gyre, WTRA; Western Tropical Atlantic; SATL; South Atlantic Subtropical gyre, SSTC; South Subtropical Convergence. The sampling stations are represented by white squares.

2. Sampling and Methodology

[6] The Atlantic Meridional Transect (AMT) was used as a platform from which to determine the variability of OVOC concentrations over a large geographical scale. The research vessel *RRS James Cook* passed through ~13,500 kilometers of Atlantic Ocean (Falmouth, UK, to Punta Arenas, Chile; 49°N to 39°S) during October to December 2009, and covered seven different Atlantic biological provinces as defined by *Longhurst* [1995]. Figure 1 shows the cruise track, provinces, and sampling stations ($n = 62$) along the transect. Sampling and analysis was therefore made across a diversity of ecosystems, from temperate and equatorial upwelled water to oligotrophic gyres [*Aiken et al*., 2000; *Robinson et al*., 2006]. Two conductivity temperature depth (CTD) casts were carried out per day, predawn and solar noon. Water was sampled from five depths at the predawn cast (5–200 m; 5 m samples used to assess surface OVOC distribution and all five depths analyzed to generate vertical profiles) and from surface only (5 m) at solar noon. Optics measurements were made to determine the levels of solar radiation at the time of each afternoon CTD cast [*Aiken et al*., 2000]. Water collected from the CTD was also analyzed for primary production [*Tilstone et al*., 2009], bacterial production (derived from bacterial leucine incorporation) [*Dixon et al*., 2011a], nutrient analysis [*Rees et al*., 2009], and flow cytometry [*Tarran et al*., 2006]. The primary production data allowed us to define whether our sampling was taking place in a gyre or more temperate waters. Overall, the highest levels of primary production were 104 mgC m^{-3} day^{-1} in the South Subtropical Convergence (SSTC) at 39°S, and the lowest in the Northern Atlantic Subtropical Gyre (NAST(W); 27°N) at 0.4 mgC m^{-3} day^{-1}.

[7] All samples analyzed for the presence of OVOCs were collected from CTD casts using 20 L stainless steel sprung Niskin bottles. Contamination by air was minimized by sampling first from the Niskin using Tygon^{TM} tubing, directly into brown glass sample bottles, to minimize the possibility of photochemical enhancement or degradation. Analysis commenced directly after sampling to minimize storage time (maximum period of ~4–4.5 h; refer to *Beale et al*. [2011] for further information). To preserve sample integrity, exposure to lab or ambient air was minimized and, where possible, samples were stored at in situ temperature. Samples were not filtered prior to analysis, as we found previously that this altered OVOC concentrations [*Beale et al*., 2011].

[8] The method used to extract and quantify OVOCs in sea water has been previously published [*Beale et al*., 2011], therefore only a brief description will be given here. We used a proton transfer reaction/mass spectrometer

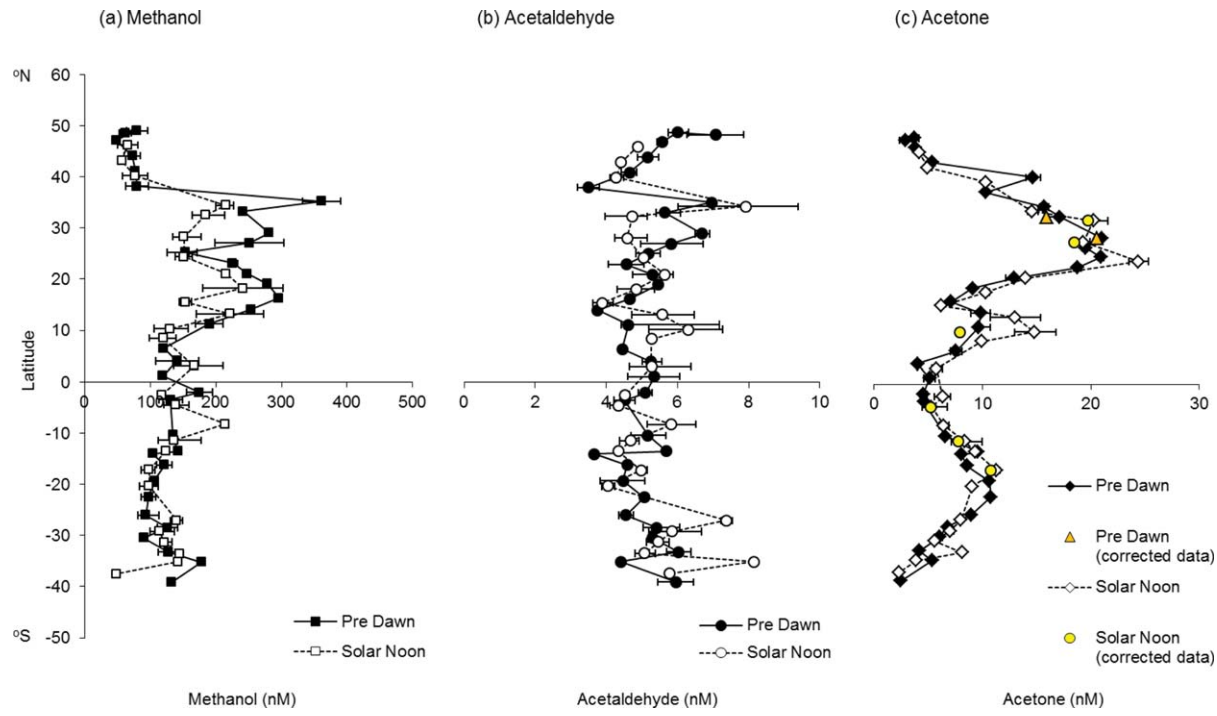

Figure 2. Sea surface (5m) concentrations during AMT19 for (a) methanol, (b) acetaldehyde and (c) acetone. Error bars represent the range of concentrations generated for each cast. Corrected data for acetone shown (in addition to uncorrected data) in (c) using concentration generated for propanal via GC/FID (see text).

(PTR/MS, high sensitivity; Ionicon, Austria). Because it is not equipped for direct aqueous injection, a membrane inlet (MI) was optimized at Plymouth Marine Laboratory and acts as an interface between the solution and the instrument inlet. There is movement of OVOCs from the seawater into the membrane gas phase (nitrogen), which is pumped directly into the PTR/MS for ionization and subsequent detection. Ionization is achieved by hydronium ions (H_3O^+) transferring a proton to the OVOC molecule in the drift tube. This creates little fragmentation, and the OVOCs are detected at their molecular weight + 1 (methanol at 33, acetaldehyde at 45, and acetone at mass 59). Solvent addition of methanol, acetaldehyde, and acetone to seawater followed by subsequent serial dilution (in seawater) generated water standards which were used for system calibration. Standards and samples were analyzed by the same technique, allowing for direct concentration comparison. Limits of detection (LODs) are calculated at 27 n*M* for methanol, 0.7 n*M* for acetaldehyde, and 0.3 n*M* for acetone. Precision of the method for all compounds was better than 10%.

[9] In addition to this technique, we also deployed a purge and trap gas chromatography–flame ionization detector (P&T-GC/FID; SRI Instruments, USA), which can identify the presence of propanal, propanol isomers, and ethanol in seawater [*Beale et al*., 2010, 2011]. Propanal is a known interferent to acetone detection via PTR/MS due to the formation of the same ion (mass 59) making them indistinguishable [*de Gouw et al*., 2003]. The contribution of propanal is assumed to be low in seawater, and thus the acetone concentration reported in previous datasets is uncorrected [*Williams et al*., 2004; *Kameyama et al*., 2010]. The analytical column we use can resolve these species, indicating when an MI-PTR/MS-derived acetone result needs to be corrected for the presence of propanal. Interference to mass 33 and 45 is considered to be low [*de Gouw et al*., 2003]. For further information on system specificity, refer to *Beale et al*. [2011]. Measurements of propanol and ethanol made using the P&T GC/FID have already been reported elsewhere [*Beale et al*., 2010].

3. Spatial OVOC Distribution

[10] Samples collected at a depth of 5 m (referred to as "surface" samples) from each cast (predawn and solar noon) were used to assess the spatial distribution of the OVOCs throughout the Atlantic Ocean. These observed surface OVOC concentrations have been plotted against latitude in Figures 2a–2c.

3.1. Surface Methanol

[11] Methanol surface concentrations ranged from 48 to 361 n*M* (Figure 2a) and demonstrated considerable spatial variability, particularly between provinces. The lowest concentrations of methanol were generally observed in the temperate waters of the North Atlantic Drift Region (NADR), off the UK coast (48–38°N). The highest concentrations were observed in the oligotrophic Northern Atlantic Gyre (35–14°N), corresponding to the lowest levels of primary production. This was unexpected, as we presumed that low biological productivity in combination with remote location (i.e., increased distance from terrestrial methanol sources) would result in low methanol concentrations. Furthermore, *Dixon et al*. [2011b] report biological turnover times as low as 1 day in surface waters of the

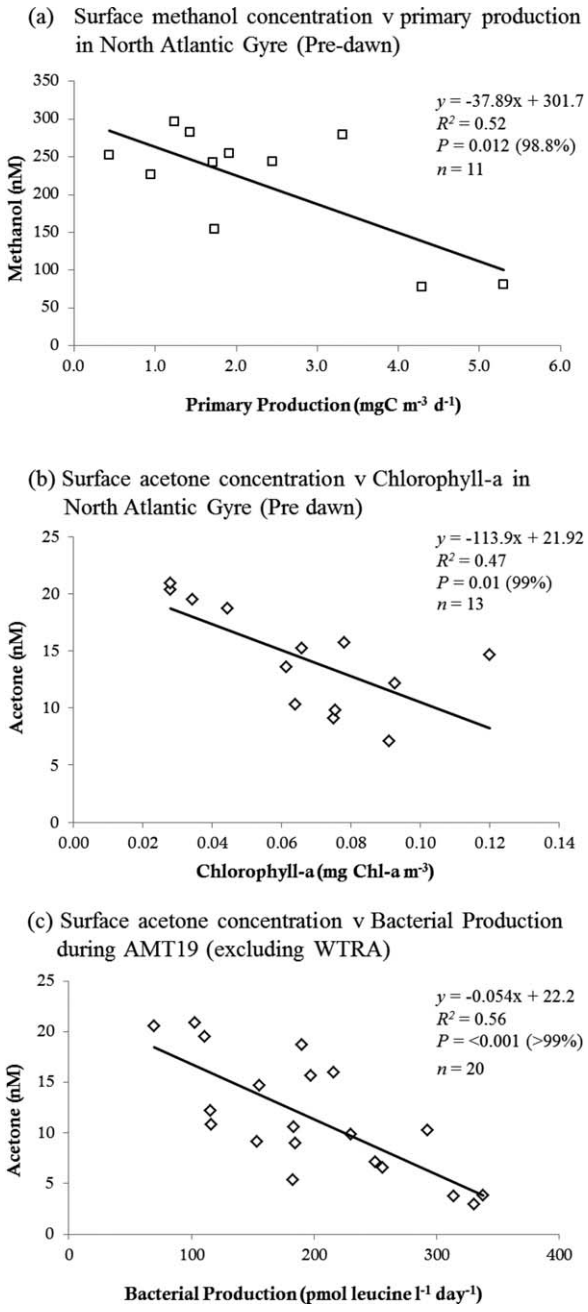

Figure 3. Statistically significant correlations observed between (a) surface methanol concentration and primary production in North Atlantic gyre (NAG); (b) surface acetone concentration and chlorophyll-a abundance in NAG (NAG comprised of the following three provinces; NAST(E), NAST(W) and NATR; refer to Figure 1); (c) surface acetone concentration and bacterial production data over AMT19 (excluding WTRA where rates were >400 pmol leucine l^{-1} day^{-1}).

oligotrophic tropical Northeast Atlantic, implying that there must be a large oceanic source in the spatially dominant North Atlantic gyre system.

[12] *Williams et al*. [2004] report a mean methanol concentration of 118 n*M* (standard deviation (σ) of 48 n*M*; $n = 210$) in the tropical Atlantic between latitudes of 0 and 10°N. Data collected in this region during AMT19 averaged 133 n*M* ($\sigma = 19$ n*M*; $n = 6$) and are therefore in good agreement with the earlier observations.

[13] The mechanism by which methanol is produced in seawater is still unconstrained. It has not been observed as a product of photochemical interactions in surface seawater. Instead it is suspected that biological production is the more likely in situ source [*Heikes et al*., 2002]. Therefore, we analyzed surface methanol concentrations for potential relationships with chlorophyll-a abundance and rates of primary and bacterial productivity using data from predawn casts. The data were also split into three large sections: the North Atlantic Gyre (NAG, comprising NAST(E), NAST(W), and NATR; refer to Figure 1; 43–13°N); the Western Tropical Atlantic (WTRA; 11°N–5°S); and the South Atlantic Subtropical Gyre (SATL; 10–35°S). Using simple regression analysis, no statistically significant relationships between surface methanol concentrations and chlorophyll-a or bacterial leucine incorporation were observed for the predawn dataset for any region. However, in the NAG, methanol did show a statistically significant negative relationship with primary production (Figure 3a), which was not observed in any other region. This suggests that in this oligotrophic region, methanol concentrations are highest when primary production rates are lowest, perhaps suggesting that methanol may be elevated due to its reduced use by phytoplankton as a carbon source. Calculations by *Dixon et al*. [2011b] suggest that methanol does contribute, on average, 13% to bacterial carbon demand (carbon required for energy and growth) in the NAG, despite the lack of correlation between the concentration of methanol in the water and bacterial leucine incorporation.

3.2. Surface Acetaldehyde

[14] In contrast to methanol, acetaldehyde concentrations show little variability over the entire transect, and range between 3 and 9 n*M* (Figure 2b). This suggests that production and consumption mechanisms driving the acetaldehyde concentrations throughout the Atlantic Ocean are more in balance compared with methanol. This may be expected as current understanding is that the two compounds are produced via different sources; acetaldehyde is associated with photochemical production [*Mopper and Stahovec*, 1986] rather than biological, like methanol. Using regression analysis, we did not observe any relationships between surface acetaldehyde concentration and either chlorophyll-a, primary production, or bacterial leucine incorporation for the entire transect, or in any of the three regions mentioned above. This implies that the concentration of acetaldehyde in the surface Atlantic Ocean is not directly linked to either heterotrophic or autotrophic carbon utilization, although we cannot rule out the possibility of microbial uptake of acetaldehyde.

[15] These observed concentrations are higher than those reported by *Kameyama et al*. [2010] for the North Pacific (<4 n*M*) and *Zhou and Mopper* [1997] from the Bahamas (1 n*M*), but are within the range of measurements reported by *Mopper and Stahovec* [1986] (3–30 n*M*) for Florida surface waters.

3.3. Surface Acetone

[16] Surface acetone concentrations ranged between 2 and 24 n*M* in the surface Atlantic Ocean (Figure 2c).

Measurements showed a progressive increase from the UK (3 n*M* at 49°N) to a maximum in the northern gyre at 24°N (24 n*M*). If the atmosphere overlying the northern gyre does not contain adequate levels to explain this trend via deposition to the surface ocean, then these data suggest that there must be a significant production mechanism for acetone occurring in these remote marine waters. Thereafter, acetone levels decreased, but did show a smaller peak of 13 n*M* at 13°N, in the equatorial upwelling region. The oligotrophic water of the Southern gyre (2–35°S) contained lower concentrations compared with the Northern Hemisphere, with a maximum of 11 n*M*. Concentrations of chlorophyll-a were low in both the northern and southern gyres, so these data alone do not explain the acetone trends observed.

[17] *Williams et al*. [2004] measured acetone in the Atlantic Ocean between latitudes of 0 and 10°N and report a mean seawater surface concentration of 18 n*M* ($\sigma = 8$ n*M*; $n = 214$). Our observations over similar latitudes (1–11°N) were lower than this, at an average value of 8 n*M* ($\sigma = 4$ n*M*; $n = 6$), despite both sets of observations being made at a similar time of year (October–November).

[18] A statistically significant negative correlation was observed between surface acetone concentrations and chlorophyll-a in the NAG (Figure 3b) which was not observed in the SATL, the WTRA, or over the full dataset. This suggests that the phytoplankton community present in the northern gyre may have utilized acetone as either an energy or a carbon source, although correlations do not necessarily imply causality.

[19] Preliminary incubation experiments on AMT19 using ^{14}C-labeled acetone, utilizing a similar approach to ^{14}C methanol [*Dixon et al*., 2011a], suggest that microbial turnover of acetone in the northern gyre is ~4.5 days. We found a statistically significant negative correlation between surface acetone concentrations and bacterial leucine uptake rates for all regions except the equatorial upwelling (Figure 3c). This suggests that heterotrophic bacteria are utilizing acetone, and thus contributing to oceanic acetone removal. Previous research indicates that heterotrophic bacteria are also capable of producing acetone [*Nemecek-Marshall et al*., 1995] and thus may be important organisms in the cycling of this OVOC. No correlations between acetone concentration and primary production were observed, suggesting that marine plankton are not a significant net source of this compound.

[20] A recent study by *Fischer et al*. [2012] attempts to assess the importance of the global oceans to the atmospheric acetone budget. The authors utilize a fixed oceanic value of 15 n*M* and only evaluate the sensitivity of the model over the range of 10–20 n*M*. These data show that surface acetone concentration in the Atlantic Ocean varied by an order of magnitude (2–24 n*M*) during our expedition. Given the high spatial variability observed, additional in situ measurements are needed to improve process models, thus enabling the role of oceanic OVOCs in atmospheric processes and composition to be further understood.

3.4. Quantifying the Contribution of Propanal to Mass 59

[21] Data generated from eight stations during AMT19 using our two independent OVOC analytical techniques are used to assess the possible contribution of propanal to mass 59 to allow a more accurate measurement of acetone concentration via PTR/MS. Comparison with propanal-spiked water standards allowed quantification of the surface concentration via P&T-GC/FID. From this, and the total nanomolar value generated by the PTR/MS, we estimate that the proportion of the mass 59 signal likely to have been attributed to acetone was typically between 93 and 98%. Thus, our measurements support the earlier assumptions made by *Williams et al*. [2004] and *Kameyama et al*. [2010] that propanal typically makes a minor contribution to the mass 59 signal. However, at 10°N, there was a large increase in propanal surface concentration, indicating that in this region, the PTR/MS signal response comprised 47% propanal and 53% acetone (assuming no other interferences). This represents a substantial correction to the acetone signal and highlights that there may be a significant error in uncorrected acetone data from some marine locations, particularly as propanal has been identified as a product of the reaction between marine DOM and sunlight [*Mopper and Stahovek*, 1986]. We have displayed both corrected and uncorrected data in Figure 2c for comparison and accept that the remainder of our uncorrected measurements may represent an upper limit for acetone concentration.

3.5. Photochemical Effects

[22] The OVOC surface data (sampled from a depth of 5 m) allowed comparison of concentrations measured in the dark (predawn, cast time typically between 04:00 and 06:00 local time) to those carried out during solar noon (typically between 12:00 and 14:00, local time) within Atlantic provinces.

[23] Surface concentrations of methanol averaged 148 n*M* ($\sigma = 76$ n*M*) and 139 n*M* ($\sigma = 51$ n*M*) for predawn and solar noon respectively, over the entire transect (Figure 2a). Statistical analysis using an independent two-tailed *t* test (at the 95% confidence level) shows that there were no significant differences between cast times over the course of the entire transect. Solar noon casts in the Northern Hemisphere exhibit consistently lower methanol concentrations than those at predawn (Figure 2a), whereas methanol concentrations in the Southern Hemisphere were similar between the two sampling times. Thus, the action of UV light on surface water in the Northern Hemisphere may have caused methanol degradation, or alternatively, biological production of methanol could have been higher during darkness (i.e., suppressed by light). Previously published experiments show that biological methanol loss processes tend to be highest predawn, and consistently decrease from dawn to dusk [*Dixon et al*., 2011b]. Thus, it is unlikely that increased biological uptake at solar noon could account for the observed concentration differences. Furthermore, we are not aware of any literature that supports the photochemical destruction (or production) of methanol by photochemical mechanisms. The results from both hemispheres highlight that there appear to be significant differences between the northern and southern oligotrophic gyres that influence methanol concentrations. Furthermore, due to the cruise progression, there is ~60 nautical miles difference between sampling at predawn and solar noon, so spatial variability may have influenced the differences observed in surface concentrations. Solar radiation levels varied with

latitude during the cruise, with light intensity highest in the Southern Hemisphere (maximum UVA and UVB intensity recorded at 24°S at 39 and 3 W/m^2, respectively).

[24] Acetaldehyde concentrations in the surface ocean when sampled predawn and solar noon were highly comparable and averaged 5.3 n*M* ($\sigma = 0.9$ n*M*) and 5.3 n*M* ($\sigma = 1.2$ n*M*), respectively, over the entire transect (Figure 2b). Statistical analysis shows that there were no significant differences between cast times (for the entire transect) or between the Northern and Southern Hemispheres (for either cast time). Previous research suggests that the ocean is supersaturated with respect to acetaldehyde and therefore the flux is in the sea-to-air direction [*Singh et al*., 2004; *Millet et al*., 2010]. The most likely in situ source of oceanic acetaldehyde is the phototransformation of humic substances, which contribute to the total DOM pool [*Mopper et al*., 1991; *Miller and Moran*, 1997; *Moran and Zepp*, 1997]. This carbonyl compound has been shown to be one of the dominant photoproducts observed from the photosensitization of DOM, along with formaldehyde, propanal, and glyoxal [*Mopper and Stahovec*, 1986]. Thus, we expected to find elevated surface concentrations of acetaldehyde at solar noon compared to predawn, and particularly in those regions where DOM precursors were highest, e.g., over the equatorial upwelling where we observed enhanced primary productivity and levels of chlorophyll-a. Therefore, either photochemistry did not significantly contribute to the production (or loss) of acetaldehyde in the surface Atlantic Ocean, or any production was balanced by loss processes (possibly microbial consumption).

[25] There were three regions (8–13°N, 27°S, and 35°S) where the solar noon concentrations were noticeably higher than those predawn (Figure 2b), suggesting that photochemistry may have influenced acetaldehyde production in these locations. Solar insolation measured at these latitudes was not higher than at other locations sampled, therefore the enhanced acetaldehyde levels observed during solar noon were more likely to have been influenced by increased levels of photoprecursors or enhanced by microbial alterations of the DOM pool. Our results disagree with the work conducted by *Zhou and Mopper* [1997] and *Mopper and Stahovec* [1986], who report diurnal variability in acetaldehyde levels with maximum concentrations reportedly observed at 14:30 [*Zhou and Mopper*, 1997] and in the late afternoon [*Mopper and Stahovec*, 1986]. Our results suggest that either the DOM photoprecursors were not present in sufficient quantities during this transect, or that any photochemically produced acetaldehyde was rapidly consumed. Preliminary microbial acetaldehyde turnover times, determined from incubations with ^{14}C-labeled acetaldehyde during AMT, suggest rapid consumption by microbes of the order of 3–6 h in the north and south temperate regions, although times in the gyres and equatorial upwelling are up to 24 h (J. Dixon, unpublished data collected in 2009), similar to methanol turnover in oligotrophic water [*Dixon et al*., 2011b]. Furthermore, *Zhou and Mopper* [1997] reported the strong diurnal cycle in microlayer samples taken from Hatchet Bay in the Bahamas, and *Kieber et al*. [1990] observed the highest photochemical production rates from DOM-rich inland and coastal waters. This may indicate that samples taken from a depth of 5 m (AMT19) are not comparable to those of the microlayer or that the remote ocean sampled during AMT19 contains less reactive DOM (particularly of terrestrial origin) such that the photochemical diurnal acetaldehyde cycle is weakened or absent.

[26] Acetone concentrations at the two cast times sampled during the transect also exhibited good similarity, with average concentrations of 9.5 n*M* ($\sigma = 5.5$ n*M*) and 9.3 n*M* ($\sigma = 4.8$ n*M*) for predawn and solar noon, respectively (Figure 2c). Acetone is also known to be produced in surface waters via the interaction of sunlight and DOM [*Miller and Moran*, 1997; *Zhou and Mopper*, 1997]. Therefore, we also expected higher acetone concentrations at solar noon, but this was not consistently observed and the data resulted in no statistically significant differences over the entire transect or for either the North or South Atlantic data. This implies that photochemistry is not a controlling mechanism on surface acetone concentrations (in these locations), unless balanced by rapid uptake/degradation. In a manner similar to acetaldehyde, we do find higher acetone concentrations at solar noon at latitudes between 13°N and the equator, which comprises the upwelling region. This could be evidence of elevated DOM precursors or enhanced biologically mediated acetone production in this more productive region. Therefore, this could show agreement with the mesocosm experiments conducted by *Sinha et al*. [2007], where a positive correlation was shown between acetone emissions to the atmosphere with photosynthetically active radiation (PAR) during a phytoplankton bloom.

4. Vertical OVOC Distribution

[27] Sample depths were selected according to light (PAR) penetration estimated from the previous noon cast. PAR refers to wavelengths of light between 400 and 700 nm in the visible region of the spectrum. Depths sampled corresponded to 97% (surface samples taken from a depth of 5 m), 33%, 14%, and 1% PAR equivalent light depths. The deepest light penetration observed during this cruise was in the Southern gyre, where 1% PAR was measured at a typical depth of 150 m. The Southern gyre is an area of low nutrients and primary production; therefore, less of the radiation is absorbed and scattered during daylight. This can be compared to 1% PAR in the NADR of ~50 m. We also sampled consistently from a depth below the euphotic zone (200 m). The data collected have been averaged ($n = 2$ per day per depth, with the exception of 97% PAR, which was typically $n = 3$) and plotted against latitude in Figures 4a–4c. The ranges observed for all three OVOCs at each light-equivalent depth are presented in Table 1.

4.1. Methanol

[28] No consistent trend in depth profiles for methanol was observed during the AMT cruise. Northern temperate (NADR), equatorial, and southern Atlantic waters sampled show little variability with depth, suggesting that either the lifetime of methanol in seawater is long (unlikely given the biological oxidation rates reported by *Dixon et al*. [2011b]) or that the rate of consumption and production was in approximate balance even down to 200 m. Recent evidence from waters bordering the NADR and NAST(E) boundaries suggests that microbial methanol oxidation rates were

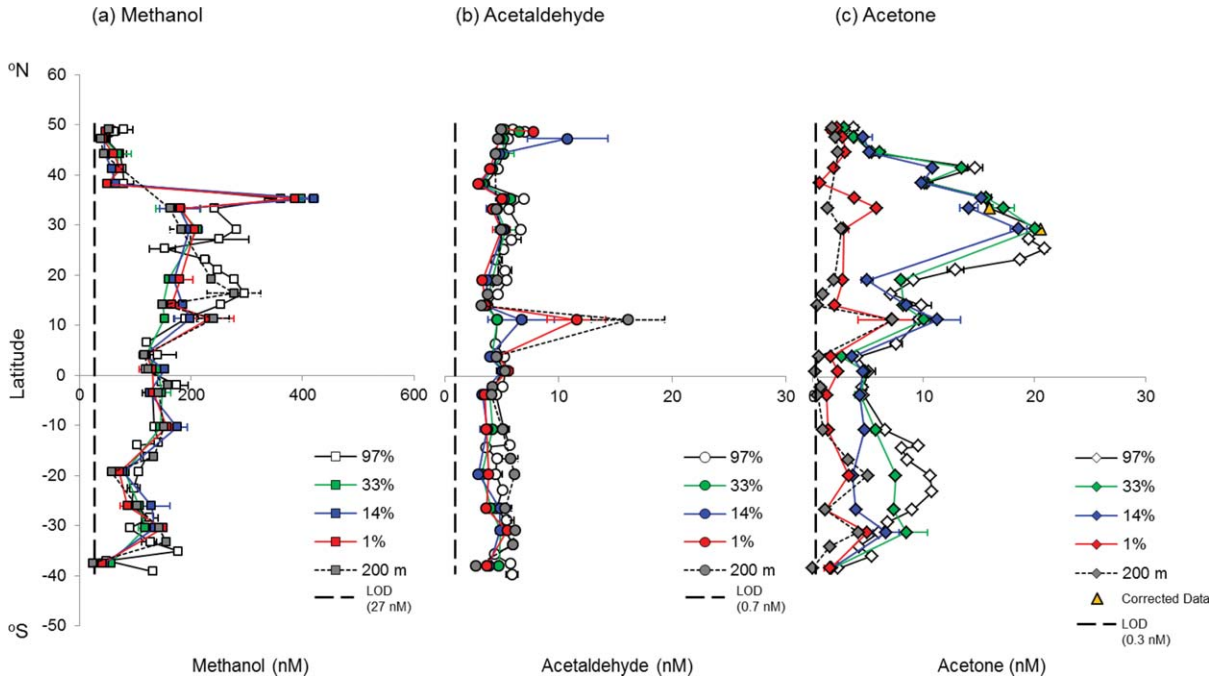

Figure 4. Average depth measurements recorded on AMT19 for 5 different light depths for (a) methanol, (b) acetaldehyde and (c) acetone. The 97 % acetone data includes propanal-corrected data where appropriate (n=2, see text). Error bars represent the range of concentrations measured for each depth along the transect. Where LOD = Limit Of Detection.

Table 1. Summary of OVOC Concentrations Observed at Each Light Equivalent Depth Sampled During AMT19[a]

PAR Equivalent Light Depth (%)	Methanol (N*m*)	Acetaldehyde (N*m*)	Acetone (N*m*)
97	48–361	3–9	2–24
33	45–398	3–7	2–20
14	43–420	3–11	2–19
1	42–387	3–12	1–7
200 m (aphotic)	<LOD –277	3–16	<LOD –7

[a]PAR, photosynthetically active radiation; LOD, limit of detection.

statistically the same from the microlayer to 1000 m [*Dixon et al*., 2012]. The northern gyre shows evidence of higher concentrations being observed in surface waters. However, for NATR waters, samples collected below the mixed layer at 200 m are also notably high in methanol (concentrations reached 277 n*M*). The methanol profiles in Figure 5 show that the maximum rate of concentration decline does not always correlate with the bottom of the mixed layer, as *Williams et al*. [2004] suggest. Subsurface maxima in methanol were often observed, consistent with either decreased

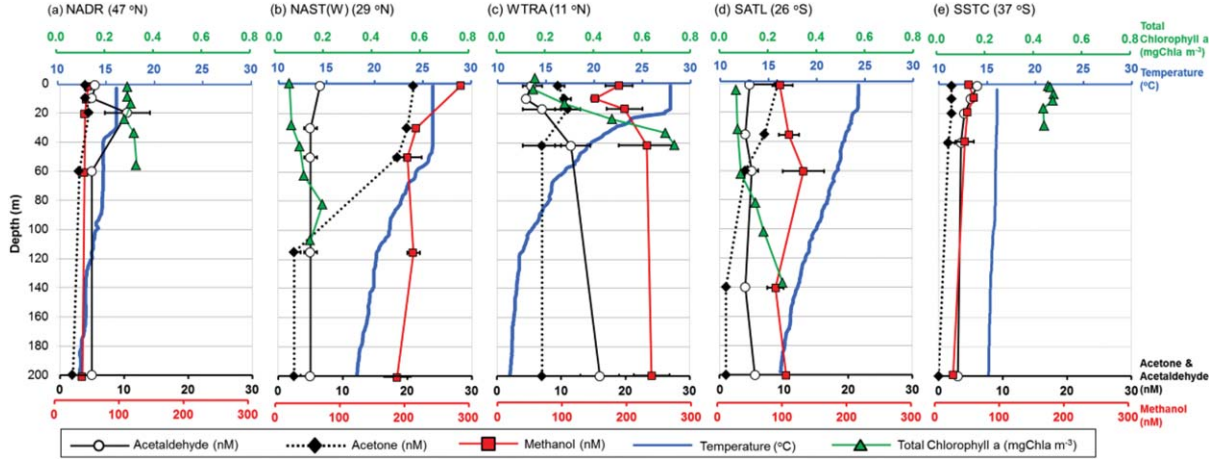

Figure 5. Typical OVOC depth profiles, temperature and chlorophyll-a measurements from (a) temperate water of the NADR; (b) oligotrophic water of the NAST(W); (c) the equatorial upwelling region of the WTRA; (d) oligotrophic water of the SATL; (e) temperate water of the SSTC (refer to Figure 1 for province description). Error bars represent the range of measurements taken for each particular depth (typically n=2).

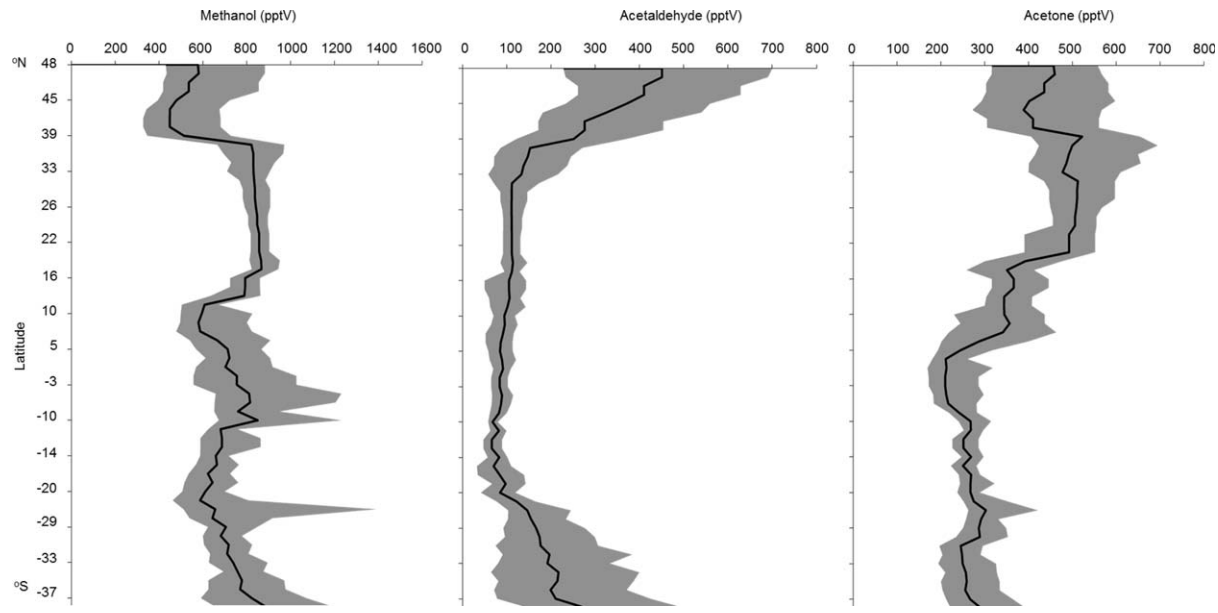

Figure 6. Modelled OVOC air concentrations (*Ca*) for AMT19. Black lines show monthly-mean concentrations from the CAM-Chem model and the shaded areas denote minimum and maximum daily mean model concentrations for the period and latitudes sampled during AMT19. Please refer to text for details of the model.

uptake/degradation (photochemical and/or microbial) or enhanced production compared with surface samples.

4.2. Acetaldehyde

[29] Acetaldehyde depth profile measurements for the transect are presented in Figures 4b and 5 and Table 1. For both the subtropical and tropical regions of the northern gyre (16–41°N), the highest acetaldehyde concentrations of 4–8 n*M* were observed in the surface ocean (97% PAR). Below this, acetaldehyde concentrations exhibited little variability with depth, as illustrated in the vertical profile at 29°N (Figure 5b). We also observed a large increase in average acetaldehyde concentration (11 n*M*) at 14% light equivalent depth at 47°N (NADR), which cannot be explained by any observed changes in chlorophyll-a abundance or primary production rates. Additionally, elevated concentrations in acetaldehyde levels were shown at depths $\leq$14% PAR equivalent depth ($\geq$17 m) at 11°N (Figure 4b). This station was in the equatorial upwelling, confirmed by the decrease in sea temperature below the mixed layer to 19°C at 1% PAR depth (compared with 28°C at 14°N and 4°N, the stations sampled on either side of 11°N) and then further to 11°C at 200 m. This station also had increased nutrient concentrations throughout the water column, presumably supplied by deeper water being upwelled. Surface levels of chlorophyll-a at 11°N are reasonably consistent with the rest of the surface data ($\sim$0.15 mgChla m^{-3}), but there is an increase below the mixed layer ($>$0.7 mgChla m^{-3}; refer to Figure 5c) that corresponds with an observed increase in acetaldehyde concentration. No direct link to phytoplankton data was observed. Our depth concentrations are similar to those of *Mopper and Kieber* [1991] from the anoxic waters of the Black Sea, who report acetaldehyde at $<$4 n*M* and most of the depth measurements (down to 200 m) are $<$ 2 nM. We note that there are different vertical trends in acetaldehyde concentration in the northern and southern gyres. In the North there was an observed decrease in concentration with depth consistent with either a reduction in production or an increase in consumption with depth. In the South the maximum concentration was often seen in the deepest samples collected (200 m). This implies that there was increased production of acetaldehyde at 200 m, or that there were reduced removal processes, or that the two gyres were simply influenced by different water masses.

4.3. Acetone

[30] Maximum acetone concentrations of up to 21 n*M* were measured in the surface (97% PAR equivalent light depth) ocean of the subtropical northern gyre. The concentrations of acetone showed remarkably little variability from the surface to the 14% PAR depth (maximum of 19 n*M*). The depth profile in Figure 5b shows that these depths are within the mixed layer at 29°N (0–45 m), below which concentration significantly decreases to $\sim$3 n*M* at 1% PAR and at 200 m. Surface water concentrations of the South Atlantic Gyre were approximately one half of those observed in the North, with a maximum of 11 n*M* at 23°S. Furthermore, enhanced variability was observed in the Southern gyre (10–35°S), with concentration decreasing to $\sim$7 n*M* ($\sigma = 1.2$ n*M*) at 33% and 5 n*M* ($\sigma = 1.4$ n*M*) at 14% PAR light depths. The temperature profile in Figure 5d shows that the mixed layer is much shallower at 26°S (0–17 m) compared with the northern gyre (29°N; Figure 5b), highlighting that the acetone concentration often follows the decrease in vertical mixing. These profiles (Figure 5) demonstrate good agreement with *Williams et al*. [2004], showing the maximum rate of concentration decline is at or close to the base of the mixed layer. In contrast to methanol and acetaldehyde, a typical trend in the acetone vertical profiles was

observed (Figure 4c), with lowest concentrations typically seen in the 1% PAR light depths and 200 m samples (maximum of ~ 5 n*M* and a minimum of below the LOD). This suggests that the oceanic lifetime of acetone may be shorter than methanol and acetaldehyde, or that in situ production/consumption mechanisms differ significantly with depth. At 11°N, the deepest samples showed relatively enhanced concentrations of acetone (7 n*M*), which may have been the effect of the upwelling region, as discussed above for acetaldehyde.

5. Gas Transfer of the OVOCs

5.1. Atmospheric OVOCs

[31] As we did not successfully make atmospheric measurements of OVOCs during AMT19, we have modeled the likely in situ marine boundary layer concentrations for the locations sampled during the period of AMT19. Monthly mean atmospheric marine boundary layer concentrations of the OVOCS are taken from a simulation using the CAM-Chem model [*Lamarque et al*., 2011]. CAM-Chem is a global model of tropospheric chemistry driven by analyzed meteorological fields and surface emissions of reactive trace gases and aerosols from anthropogenic, biogenic, and biomass burning sources. The use of analyzed meteorology means that the atmospheric transport of trace gases and aerosol species is constrained to observed global meteorology over the time period of the simulation. The model has been adapted to include bidirectional oceanic fluxes of the OVOC species [*Read et al*., 2012], consistent with the OVOC seawater abundances in this study. For further details on the model and simulations, see *Read et al*. [2012]. The modeled OVOC air concentrations at the locations of the water sampling are shown in Figure 6. For methanol the concentrations are similar to those previously reported over the Atlantic Ocean. The average simulated air concentration for this time period was 0.7 ppb, which can be compared to measurements of 0.9, 0.9, and 0.6 ppb reported by *Heikes et al*. [2002], *Williams et al*. [2004], and *Jacob et al*. [2005], respectively. The average simulated acetaldehyde air-side concentration (0.2 ppb) is lower than that reported by *Lewis et al*. [2005] (0.4 ppb) at Mace Head. This is consistent with a large-scale underestimate in modeled acetaldehyde concentrations in the remote atmosphere as shown in previous global modeling studies [*Staudt et al*., 2003; *Singh et al*., 2004; *Millet et al*., 2010]. Comparison of the model with multiseasonal concentrations measured at the Cape Verde Atmospheric Observatory in the tropical Atlantic [*Read et al*., 2012] suggests that even with ocean fluxes implemented, the CAM-Chem model likely underestimates acetaldehyde in this region by a factor of 4. Our simulated acetone atmospheric concentration (average of 0.3 ppb) is comparable to that reported over the Atlantic Ocean by *Williams et al*. [2004] of 0.5 ppb.

5.2 Air-Sea Transfer of OVOCs During AMT19

[32] The net air-sea fluxes (F) were estimated from our measured seawater concentrations (C_w) (all 5 m samples, from predawn and solar noon casts) and the modeled atmospheric concentrations (C_a) using the following expression [*Liss and Slater*, 1974]:

$$F = K_t\left(\left(\frac{C_a}{H}\right) - C_w\right) \quad (1)$$

where K_t is the total gas transfer velocity and $1/K_t$ is equal to $1/k_w + 1/Hk_a$. The terms k_w and k_a are gas transfer velocities for both water and air, respectively. H denotes the Henry's law constant (corrected for salinity and temperature). The k_a and k_w values are calculated using equation (2) [*Duce et al*., 1991] and equation (3) [*Nightingale et al*., 2000], respectively:

$$k_a = \frac{u_{10}}{770 + 45 \times MW^{1/3}} \quad (2)$$

$$k_w = \left(0.222 * u_{10}^2 + 0.333 * u_{10}\right)\left(\frac{Sc_w}{Sc_{600}}\right)^{-0.5}$$

[33] where u_{10} is the average wind speed (calculated over the period of each cast), MW is the molecular weight of the OVOC, Sc_w is the Schmidt number of the gas of interest at the temperature and salinity of the sample (ratio of the kinematic viscosity of seawater (ν) and molecular diffusivity (D) of the gas in seawater), and Sc_{600} is the Schmidt number of CO_2 at 20°C in freshwater [*Nightingale*, 2000]. There are different parameterizations available for estimation of k_w. *Nightingale et al*. [2000] was chosen as the "average" prediction relative to other parameterizations [*Carpenter et al*., 2012], making it more commonly used for deriving water-side transfer velocity. Uncertainty in the flux measurements associated with the use of this parameterization is discussed later.

[34] The air-sea exchange for methanol calculated for the cruise transect is presented in Figure 7a. The range of calculated flux values spans −29 to 19 μmol m^{-2} day^{-1}, where a negative value is indicative of an oceanic source (loss of OVOC to the atmosphere). The calculations predict both an oceanic source (northern gyre) and sink (north and south temperate zones) of methanol to the atmosphere. This is in agreement with the work conducted by *Sjostedt et al*. [2012] further north of these data, who predict that the high latitudes of the Arctic Ocean act as a sink for methanol. Furthermore, methanol exchange in both directions agrees with both *Heikes et al*. [2002] and *Millet et al*. [2008]. Maximum deposition was calculated for the SSTC (38°S) and the highest emission from the ocean in the NAG (13°N). The large fluctuations in the Northern Hemisphere create an average emission flux of −6 μmol m^{-2} day^{-1} ($\sigma = 10$ μmol m^{-2} day^{-1}), and this can be compared to a sink in the Southern Hemisphere of 1 μmol m^{-2} day^{-1} ($\sigma = 5$ μmol m^{-2} day^{-1}).

[35] The magnitude of the acetaldehyde flux ranged between −9 (oceanic source) and 4 (oceanic sink) μmol m^{-2} day^{-1}. The flux direction is predominantly from the ocean to the atmosphere (Figure 7c) as predicted by published literature [*Singh et al*., 2004; *Millet et al*., 2010]. However, our calculations suggest that the ocean may also exhibit regions of under-saturation, causing the direction of the net flux to reverse, particularly at the high northern latitudes sampled (>38°N). A state of under-saturation is likely to be created through either solar degradation or biological turnover. But as predawn data also exhibit this trend, the latter is proposed as the more likely cause,

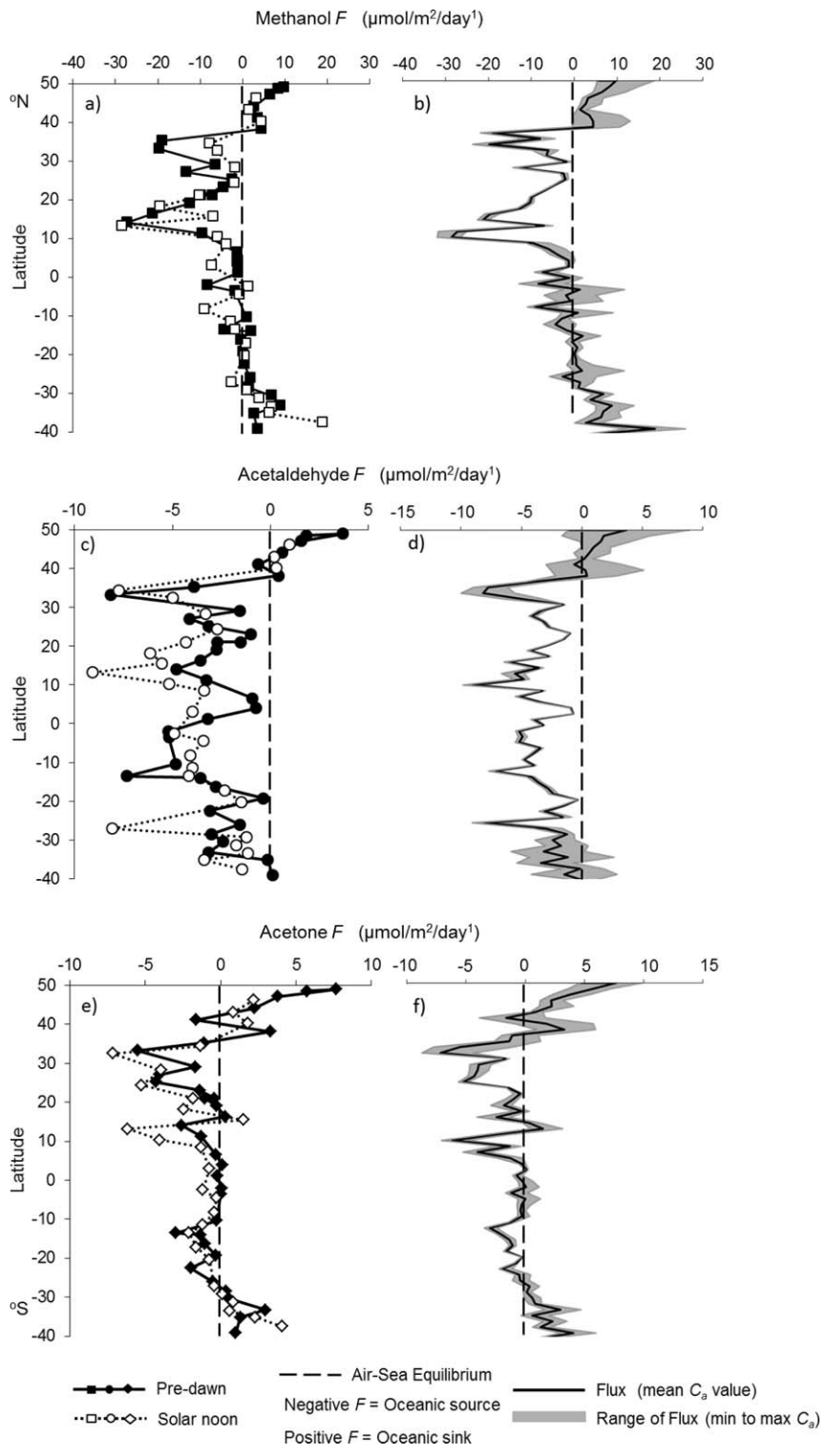

Figure 7. Direction and magnitude of the OVOC air-sea gas exchange (*F*) estimated during AMT19 using modelled air data and measured seawater concentrations for a) methanol; pre-dawn verses solar noon (using mean modelled *Ca*); b) methanol (all surface data); range of flux calculated by applying minimum and maximum modelled *Ca* values; c) acetaldehyde; pre-dawn verses solar noon flux (using mean modelled *Ca*); d) Acetaldehyde (all surface data); range of flux calculated by applying minimum and maximum modelled *Ca* values; e) acetone; pre-dawn verses solar noon flux (using mean modelled *Ca*); f) Acetone (all surface data); range of flux calculated by applying minimum and maximum modelled *Ca* values. Please refer to text for equations and parameters used to calculate *F*. Where a negative flux represents loss of OVOC from the ocean to the atmosphere and a positive flux is indicative of atmospheric deposition to the ocean.

Table 2. Extrapolation of OVOC Fluxes to Atlantic Ocean, to Provinces Sampled During AMT19, and to the Global Oceans[a]

Zone/Cast Time	Area[b] (km^2)	Methanol ($Tg\ yr^{-1}$)	Acetaldehyde ($Tg\ yr^{-1}$)	Acetone ($Tg\ yr^{-1}$)
Predawn	74.8×10^6	−3	−3	−0.2
Solar Noon	74.8×10^6	−2	−4	−2
NADR	3.5×10^6	0.2	0.1	0.3
NAG[c]	5.4×10^6	−1	−1	−1
WTRA	5.4×10^6	−0.2	−0.3	−0.1
SATL	17.8×10^6	0.2	−1	−0.2
SSTC	4.1×10^6	0.4	−0.1	0.2
Atlantic Ocean[d]	74.8×10^6	−3	−3	−1
Global oceans[d]	3.6×10^8	−12	−17	−4

[a]A negative result indicates sea-to-air flux (oceanic source), and a positive result indicates air-to-sea flux (oceanic sink); NADR, North Atlantic Drift Region; NAG, Northern Atlantic Gyre; WTRA, Western Tropical Atlantic; SATL, South Atlantic Subtropical Gyre; SSTC, South Subtropical Convergence.

[b]Area of the Atlantic Ocean is taken as 74.8×10^6 km^2 [*Takahashi et al*., 2009]; areas of each province are used to calculate annual flux [*Forster et al*., 2009]; area of 3.6×10^8 km^2 is used as the value for surface area of the Earth covered by water [*Charette and Smith*, 2010].

[c]NAG is composed of three individual provinces: North Atlantic Subtropical Gyre (East), North Atlantic Subtropical Gyre (West), and North Atlantic Tropical Gyre (as defined by *Longhurst* [1995]).

[d]Extrapolations to the Atlantic Ocean and the global oceans have been calculated simply, using the average flux for the entire AMT19 dataset (−2.86, −2.85, and −0.53 $\mu mol\ m^{-2}\ day^{-1}$ for methanol, acetaldehyde, and acetone, respectively) and the relevant area.

particularly as we report here (see earlier) preliminary measurements of acetaldehyde microbial consumption. An enhanced flux to the atmosphere at solar noon, particularly in the tropical northern gyre (0–23°N), is shown, but this is not consistent throughout the entire transect.

[36] In agreement with other published datasets [e.g., *Marandino et al*., 2005; *Sinha et al*., 2007; *Jacob et al*., 2002; *Fisher et al*., 2012], we also find both a source and sink for acetone with calculated fluxes of between −7 (oceanic source) and 8 (oceanic sink) $\mu mol\ m^{-2}\ day^{-1}$ (Figure 7e). Elevated emission of acetone from the ocean to the atmosphere is found in the Northern Hemisphere (8–33°N), with enhanced fluxes often shown at solar noon. The direction of acetone air-sea flux with respect to latitude is similar to the work of *Fisher et al*. [2012], who predict an oceanic source between 20°N and 40°S. Our acetone data predict an oceanic source from 34°N to 26°S, south of which (>26°S–39°S) we report an oceanic sink. Both datasets predict an oceanic sink at the higher northern latitudes. *Fisher et al*. [2012] suggest that this is due to elevated air concentrations influenced by Northern Hemisphere continents (in combination with cooler temperatures and stronger winds). Our results suggest that continental outflow ensures that atmospheric acetone remains sufficiently elevated over the mid-latitude North Atlantic to maintain a net ocean sink in this region. In addition, there may be a role for in situ oceanic removal processes resulting in areas of oceanic under-saturation in these more productive regions (>38°N and >27°S), further enhancing acetone flux to the oceans.

[37] Sensitivity of these OVOC air-sea fluxes to the predicted air-side concentrations is investigated by conducting additional flux calculations using the minimum and maximum daily average model atmospheric concentrations, shown in Figure 6, and comparing with those using the monthly mean atmospheric concentrations. For methanol (Figure 7b), the range of fluxes becomes −32 to 26 $\mu mol\ m^{-2}\ day^{-1}$. The highest sensitivity to the air-side concentrations are predicted in the Southern Hemisphere (<30°S), where use of the minimum C_a values results in a predominantly negative flux (oceanic source) and maximum C_a values reverse the direction so that the ocean would become largely a methanol reservoir. For acetaldehyde (Figure 7d), the range becomes −10 to 9 $\mu mol\ m^{-2}\ day^{-1}$. We believe that the model is likely to underestimate atmospheric acetaldehyde in some locations (see previous text), and applying the maximum C_a values results in an oceanic sink at the higher southern latitudes (>31°S) in addition to increasing the rate of deposition to the surface ocean between 38°N and 49°N. For acetone, there is minimal uncertainty relating to the flux estimations created by the modeled C_a values, shown in Figure 7f. The range of flux (−9 to 10 $\mu mol\ m^{-2}\ day^{-1}$) shows little fluctuation when the minimum and maximum C_a values are applied, with no change to the direction of gas transfer; the oligotrophic gyres remain a source to the atmosphere, and at the higher latitudes, a sink. In general, there is a larger range in modeled daily C_a values in the extratropical/mid-latitudes (>30°N and >30°S). At these latitudes, westerly flow from continental regions carries OVOCs and their precursors to the location of the cruise. This transport shows a high degree of day-to-day variability associated with the occurrence of extratropical cyclones and their associated frontal systems.

[38] A lesser source of uncertainty in our estimated flux rates is our use of *Nightingale et al*.'s [2000] parameterization to estimate k_w. This was derived from dual-tracer field measurements using gases much less soluble than the OVOCs studied here. The effect of bubble-mediated gas transfer is important for less soluble gases but less so for OVOCs, so *Nightingale et al*. [2000] potentially overestimate k_w. However, although real, any effect is probably small because the wind speed regime on the AMT19 cruise was low to moderate (average 7.0 $m\ s^{-1}$, range 1.4–13.6 $m\ s^{-1}$) where bubble effects on gas exchange are less important than at higher wind speeds [e.g., see *Bell et al*., 2013]. In addition, the high solubility of the OVOCs means that the majority of the resistance to gas exchange is in the air phase [*Beale*, 2011; *Rowe et al*., 2011], thus minimizing the importance of any errors in deriving k_w from *Nightingale et al*. [2000].

5.3. Global Extrapolations

[39] Fluxes were extrapolated to estimate oceanic OVOC sources and sinks for individual Atlantic provinces covered during the AMT (Table 2). Mean overall flux rates from AMT (−2.86, −2.85, and −0.53 $\mu mol\ m^{-2}\ day^{-1}$ for methanol, acetaldehyde, and acetone, respectively) are used to extrapolate to the entire Atlantic Ocean, recognizing that this is an estimate based on limited area (49°N and 39°S) and season. We also extrapolate our average fluxes to the global oceans (using the area from Table 2) as a means of a "best estimate" global budget from this limited dataset.

[40] Our calculations predict that overall the Atlantic Ocean emits 3 Tg of methanol per year to the atmosphere,

Table 3. Comparison of Annual Global OVOC Source and Sink Budgets for Oceanic Data[a]

Methanol, CH_3OH		Acetaldehyde, CH_3CHO		Acetone, $CH_3C(O)CH_3$	
Oceanic source (Tg yr^{-1})					
<0.1	*Galbally and Kirstine* [2002]	75–175	*Singh et al*. [2004]	27	*Jacob et al*. [2002]
0–80	*Heikeset al*. [2002]	57	*Millet et al*. [2010]	0–15	*Singh et al*. [2004]
85	*Millet et al*. [2008]	17	*Beale et al*. (all AMT19 data)	3	*Sinha et al*. [2007]
12	*Beale et al*. (all AMT19 data)	1–53	*Beale et al*. [this work][a]	4	*Beale et al*. (all AMT19 data)
2–121	*Beale et al*. [this work][a]			2–55	*Beale et al*. [this work][a]
Oceanic sink (Tg yr^{-1})					
0.3	*Galbally and Kirstine* [2002]	1–21	*Beale et al*. [this work][b]	14	*Jacob et al*. [2002]
85	*Heikes et al*. [2002]			14	*Singh et al*. [2003]
8	*Singh et al*. [2003]			29–67	*Marandino et al*. [2005]
15	*Singh et al*. [2004]			0.7	*Sinha et al*. [2007]
10	*Jacob et al*. [2005]			2	*Fisher et al*. [2012]
3	*Sinha et al*. [2007]			1–59	*Beale et al*. [this work][b]
101	*Millet et al*. [2008]				
0–79	*Beale et al*. [this work][b]				

Data extrapolated to the global scale.
[a]Range of lowest to highest source fluxes.
[b]Range of lowest to highest sink fluxes.

which increases to 12 Tg yr^{-1} when we extrapolate to the global oceans (product of mean flux and area from Table 2). This oceanic source is similar in strength to that of anthropogenic emissions [*Heikes et al*., 2002; *Jacob et al*., 2005]. A current summary of published global OVOC budgets is presented in *Carpenter et al*. [2012]. Our work is one of the few that has estimated oceanic budgets from in situ water measurements as opposed to assuming a set surface concentration; we compare this approach to budgets estimated in previous publications by updating *Carpenter et al*.'s [2012] table in our Table 3. For methanol, the source range agrees well with that published by *Heikes et al*. [2002] and *Millet et al*. [2008], but our "best" estimate of 12 Tg yr^{-1} is considerably lower. Our deposition rates encompass most of the previous methanol sink estimates.

[41] We estimate that the Atlantic Ocean releases 3 Tg of acetaldehyde per year into the atmosphere on an annual basis. Of the five provinces for which acetaldehyde extrapolation has been made in this work, the NADR is the only location to result in an overall under-saturation, the first suggestion that part of the oceans may act as a sink for acetaldehyde. Assuming that the Atlantic Ocean is representative of the rest of the global oceans, this marine source strength increases to 17 Tg yr^{-1}, a value close to that predicted by *Millet et al*. [2010] for primary terrestrial biogenic emissions. This oceanic source is, however, less than that predicted by *Millet et al*. [2010] and may be an indication that the Atlantic Ocean emits less acetaldehyde than other oceanic basins.

[42] These data predict that the Atlantic Ocean emits acetone to the marine boundary layer at a rate of 1 Tg of acetone per year. Extrapolating to the global oceans increases this value to 4 Tg yr^{-1} (Table 2). This prediction is comparable to the acetone released yearly from anthropogenic sources [*Jacob et al*., 2002; *Singh et al*., 2004]. Our results are in agreement with *Jacob et al*. [2002] and *Taddei et al*. [2009], who predict that the oceans are able to act as both a source and a sink of acetone (Table 3), and who also propose that exchange is from the sea to atmosphere (oceanic source) in the tropics. Again, our overall extrapolated oceanic source is lower than that predicted by *Jacob et al*. [2002] and in contrast to *Taddei et al*. [2009], who speculate that the global oceans are a net sink for acetone.

[43] We accept that these results of the extrapolation calculations (Table 2) are subject to uncertainty due to the fact that, although AMT19 had significantly greater latitudinal coverage than most research cruises, it still covered only a limited area (particularly longitudinally) of the Atlantic and had limited seasonality. Thus, our calculations should be regarded as order of magnitude indications of the fluxes from the Atlantic and global oceans. Their value is that they are more data rich than previous attempts and do serve to highlight agreement and discrepancies when compared with other (mostly modeled) approaches (Table 3).

6. Conclusions

[44] We have investigated both latitudinal and vertical distributions of OVOCs for a large part of the Atlantic Ocean. The abundance of both methanol and acetone in surface seawater fluctuated considerably with Atlantic province, suggesting that concentration is directly influenced by in situ processes and not just air-sea transfer. Acetaldehyde concentrations over the entire transect showed less variability, perhaps suggesting that production and loss processes stayed more in balance. There was no consistent relationship between any OVOC concentration and either chlorophyll-a or primary production. We can infer from this that neither of these two variables can be consistently used as a proxy for OVOC abundance.

[45] A significant relationship between surface acetone concentration and bacterial production was observed for all regions of the Atlantic Ocean (except WTRA), providing the first indication that bacteria may significantly influence acetone concentrations in surface seawater. Radiolabeled experiments showed the microbial turnover of acetone in the northern gyre to be ~4.5 days. Although the biological turnover of acetaldehyde remains unconstrained, rapid microbial consumption (0.86 h^{-1}) has been shown previously by *Mopper and Stahovec* [1986] and is supported by our

preliminary data (0.3–1 h^{-1}); therefore, we propose that this represents a realistic oceanic sink for this compound.

[46] Depth profiles presented here provide evidence that the OVOCs are not only prevalent in surface waters but are also present at depths beneath the surface mixed layer, a feature which is consistent throughout the Atlantic Ocean, particularly for methanol and acetaldehyde. In contrast, acetone concentrations drop close to our limit of detection at depths below the mixed layer.

[47] Modeled atmospheric concentrations and our surface seawater data have been used to show methanol and acetone supersaturation in the surface water, but we are currently unable to identify their sources. Overall, an oceanic emission of acetaldehyde to the atmosphere was deduced, consistent with previously published literature. However, we have also presented novel data to suggest that the Atlantic Ocean may also act as an acetaldehyde reservoir in northern temperate waters. The data are used to determine a best estimate of air-sea fluxes in order to evaluate the role of the Atlantic Ocean in the cycling of methanol, acetaldehyde, and acetone. The Atlantic Ocean represents a modest overall source to the atmosphere for all three OVOCs. Our extrapolated estimates of the global marine source of methanol, acetaldehyde, and acetone are lower than recent estimates derived from global models [*Millet et al*., 2008, 2010; *Jacob et al*., 2002], suggesting either that oceans other than the Atlantic may exhibit a stronger OVOC emission to the atmosphere or that global oceanic budgets have been previously overestimated.

[48] We have presented evidence to suggest significant biogeochemical cycling of OVOCs in the ocean. Further research is required to establish an enhanced understanding of the processes that drive the production and destruction of these trace gases in seawater.

[49] **Acknowledgments.** We thank the officers and crew of the *RRS James Cook* and the Chief Scientist Andrew Rees (Plymouth Marine Laboratory (PML)), Neil Sloane for assistance with analytical instrumentation, Claire Widdicombe (PML) for chlorophyll-a and primary production data, Glen Tarran (PML) for flow cytometry data, Carolyn Harris/Andrew Rees (PML) for nutrient data, Tim Smyth (PML) for optics data, and Stephanie Sargeant (PML) for bacterial production data. We also thank Eric Saltzman for his comprehensive review and anonymous reviewer 2. This work was funded by Oceans 2025 and UK SOLAS. This is contribution number 213 of the AMT program, a contribution to the international IMBER project supported by UK Natural Environment Research Council National Capability funding to PML and the National Oceanography Centre, Southampton.

References

Aiken, J., N. Rees, S. Hooker, P. Holligan, A. Bale, D. Robins, G. Moore, and D. Pilgrim (2000), The Atlantic Meridional Transect: Overview and synthesis of data, *Prog. Oceanogr.*, *45*, 257–312.

Arnold, F., V. Burger, B. Droste-Franke, F. Grimm, A. Krieger, J. Schneider, and T. Stilp (1997), Acetone in the upper troposphere and lower stratosphere: impact on trace gases and aerosols, *Geophys. Res. Lett.*, *24*(23), 3017–3020.

Arnold, S. R., M. P. Chipperfield, and M. A. Blitz (2005), A three-dimensional model study of the effect of new temperature-dependent quantum yields for acetone photolysis, *J. Geophys. Res. Atmos.*, *110*, D22305, doi:10.1029/2005JD005998.

Atkinson, R. (2000), Atmospheric chemistry of VOCs and NO_x, *Atmos. Environ.*, *34*, 2063–2101.

Beale, R. (2011), Quantification of oxygenated volatile organic compounds in seawater, PhD thesis, Univ. of East Anglia.

Beale, R., P. S. Liss, and P. D. Nightingale (2010), First oceanic measurements of ethanol and propanol, *Geophys. Res. Lett.*, *37*, L24607, doi:10.1029/2010GL045534.

Beale, R., P. S. Liss, J. L. Dixon, and P. D. Nightingale (2011), Quantification of oxygenated volatile organic compounds in seawater by membrane inlet—Proton transfer reaction/mass spectrometry, *Anal. Chim. Acta.*, *706*, 128–134.

Bell, T. G., W. De Bruyn, S. D. Miller, B. Ward, K. Christensen, and E. S. Saltzman (2013), Air/sea DMS gas transfer in the North Atlantic, *Atmos. Chem. Phys. Discuss.*, *13*, 13,285–13,322, doi:10.5194/acpd-13-13285-2013.

Blitz, M. A., D. E. Heard, M. J. Pilling, S. R. Arnold, and M. P. Chipperfield (2004), Pressure and temperature-dependent quantum yields for the photodissociation of acetone between 279 and 327.5 nm, *Geophys. Res. Lett.*, *31*, L06111, doi:10.1029/2003GL018793.

Carpenter, L. J., S. D. Archer, and R. Beale (2012), Ocean-atmosphere trace gas exchange, *Chem. Soc. Rev.*, *41*, 6473–6506, doi: 10.1039/c2cs35121h.

Charette, M. A., and W. H. F. Smith (2010), The volume of Earth's ocean, *Oceanography*, *23*(2), 112–114.

Chisholm S. W., R. J. Olson, E. R. Zettler, R. Goericke, J. B. Waterbury, and N. A. Welschmeyer (1988), A novel free-living prochlorophyte abundant in the oceanic euphotic zone, *Nature*, *334*, 340–343.

de Gouw, J. A., C. Warneke, D. D. Parrish, J. S. Holloway, M. Trainer, and F. C. Fehsenfeld (2003), Emission sources and ocean uptake of acetonitrile (CH_3CN) in the atmosphere, *J. Geophys. Res.*, *108*(D11), 4329, doi:10.1029/2002JD002897.

Dixon, J. L., and P. D. Nightingale (2012), Fine scale variability in methanol uptake and oxidation: from the microlayer to 1000m, *Biogeosciences*, *9*, 1–12.

Dixon, J. L., R. Beale, and P. D. Nightingale (2011a), Microbial methanol uptake in northeast Atlantic waters, *ISME J.*, *5*, 704–716, doi:10.1038/ismej.2010.169.

Dixon, J. L., R. Beale, and P. D. Nightingale (2011b), Rapid biological oxidation of methanol in the tropical Atlantic; significance as a microbial carbon source, *Biogeosciences*, *8*, 1–10.

Duce, R. A., et al. (1991), The atmospheric input of trace species to the world ocean, *Global Biogeochem. Cycles*, *5*, 193–259.

Fischer, E. V., D. J. Jacob, D. B. Millet, R. M. Yantosca, and J. Mao (2012), The role of the ocean in the global budget of acetone, *Geophys. Res. Lett.*, *39*, L01807, doi:10.1029/2011GL050086.

Forster, G., R. C. Upstill-Goddard, N. Gist, C. Robinson, G. Uher, and E. M. S. Woodward (2009), Nitrous oxide and methane in the Atlantic Ocean between 50°N and 52°S: latitudinal distribution and sea-to-air flux, *Deep Sea Res., Part II*, *56*, 964–976.

Galbally, I., and W. Kirstine (2002), The production of methanol by flowering plants and the global cycle of methanol, *J. Atmos. Chem.*, *43*, 195–229.

Hartmann M, C. Grob, G. A. Tarran, A. P. Martin, P. H. Burkhill, D. J. Scanlan, and M. V. Zubkov (2012), Mixotrophic basis of Atlantic oligotrophic ecosystems, *Proc. Natl. Acad. Sci. U. S. A.*, *109*, 5756–5760.

Heikes, B. G., et al. (2002), Atmospheric methanol budget and ocean implication, *Global Biogeochem. Cycles*, *16*, 80–113.

Jacob, D. J., B. D. Field, E. M. Jin, I. Bey, Q. Li, J. A. Logan, and R. M. Yantosca (2002), Atmospheric budget of acetone, *J. Geophys. Res.*, *107*(D10), 5-1–5–17.

Jacob, D. J., B. D. Field, Q. Li, D. R. Blake, J. de Gouw, C. Warneke, A. Hansel, A. Wisthaler, and H. B. Singh (2005), Global budget of methanol: constraints from atmospheric observations, *J. Geophys. Res.*, *110*, D08303, doi:10.1029/2004JD005172.

Kameyama, S., H. Tanimoto, S. Inomata, U. Tsunogai, A. Ooki, S. Takeda, H. Obata, A. Tsuda, and M. Uematsu (2010), High-resolution measurement of multiple volatile organic compounds dissolved in seawater using equilibrator inlet-proton transfer reaction-mass spectrometry (EI-PTR-MS), *Mar. Chem.*, *122*, 59–73.

Kieber, R. J., X. Zhou, and K. Mopper (1990), Formation of carbonyl compounds from UV-induced photodegradation of humic substances in natural waters: Fate of riverine carbon in the sea, *Limnol. Oceanogr.*, *35*, 1503–1515.

Lamarque, J.-F., et al. (2011), CAM-chem: Description and evaluation of interactive atmospheric chemistry in CESM, *Geosci. Model Dev. Discuss.*, *4*, 2199–2278, doi:10.5194/gmdd-4-2199-2011.

Lewis, A. C., J. R. Hopkins, L. J. Carpenter, J. Stanton, K. A. Read, M. J. Pilling (2005), Sources and sinks of acetone, methanol, and acetaldehyde in North Atlantic marine air, *Atmos. Chem. Phys.*, *5*, 1963–1974.

Liss, P. S., and P. G. Slater (1974), Flux of gases across the air-sea interface, *Nature*, *247*(5438), 181–184.

Longhurst, A. (1995), Seasonal cycles of pelagic production and consumption, *Prog. Oceanogr.*, *36*, 77–167.

Marandino, C. A., W. J. De Bruyn, S. D. Miller, M. J. Prather, and E. S. Saltzman (2005), Oceanic uptake and the global atmospheric acetone budget, *Geophys. Res. Lett.*, *32*, L15806, doi:10.1029/2005GL023285.

Miller, W. L., and M. A. Moran (1997), Interaction of photochemical and microbial processes in the degradation of refractory dissolved organic matter from a coastal marine environment, *Limnol. Oceanogr.*, *42*(6), 1317–1324.

Millet, D. B., et al. (2008), New constraints on terrestrial and oceanic sources of atmospheric methanol, *Atmos. Chem. Phys. Discuss.*, *8*, 7609–7655.

Millet, D. B., et al. (2010), Global atmospheric budget of acetaldehyde: 3-D model analysis and constraints from *in situ* and satellite observations, *Atmos. Chem. Phys.*, *10*, 3405–3425.

Mopper, K., and D. J. Kieber (1991), Distribution and biological turnover of dissolved organic compounds in the water column of the Black Sea, *Deep Sea Res.*, *38*, S1021–S1047.

Mopper, K., and W. L. Stahovec (1986), Sources and sinks of low molecular weight organic carbonyl compounds in seawater, *Mar. Chem.*, *19*, 305–321.

Mopper, K., X. Zhou, R. J. Kieber, D. J. Kieber, R. J. Sikorski, and R. D. Jones (1991), Photochemical degradation of dissolved organic carbon and its impact on the oceanic carbon cycle, *Nature*, *353*, 60–62.

Moran, M. A., and R. G. Zepp (1997), Role of photoreactions in the formation of biologically labile compounds from dissolved organic matter, *Limnol. Oceanogr.*, *42*, 1307–1316.

Nemecek-Marshall, M., C. Wojciechowski, J. Kuzma, G. M. Silver, and R. Fall (1995), Marine vibrio species produce the volatile organic compound acetone, *Appl. Environ. Microbiol.*, *61*, 44–47.

Nightingale, P. D., G. Malin, C. S. Law, A. J. Watson, P. S. Liss, M. I. Liddicoat, J. Boutin, and R. C. Upstill-Goddard (2000), In situ evaluation of air-sea gas exchange parameterizations using novel conservative and volatile tracers, *Global Biogeochem. Cycles*, *14*, 373–387.

Read K, L. J. Carpenter, S. Arnold, R. Beale, P. D. Nightingale, J. R. Hopkins, A. C. Lewis, J. D. Lee, L. Mendes, and S. J. Pickering (2012), Multi-annual observations of acetone, methanol and acetaldehyde in remote tropical Atlantic air: Implications for atmospheric OVOC budgets and oxidative capacity, *Environ. Sci. Technol.*, *46*, 11028–11039.

Rees, A. P., E. M. S. Woodward, and I. R. Joint (2006), Concentrations and uptake of nitrate and ammonium in the Atlantic Ocean between 60°N and 53°S, *Deep Sea Res., Part II*, *53*, 1649–1665.

Robinson, C., et al. (2006), The Atlantic Meridional Transect (AMT) programme: a contextual view 1995–2005, *Deep Sea Res., Part II*, *53*, 1485–1515.

Rosado-Reyes, C. M., and J. S. Francisco (2007), Atmospheric oxidation pathways of propane and its by-products: Acetone, acetaldehyde, and propionaldehyde, *J. Geophys. Res.*, *112*, D14310, doi:10.1029/2006JD007566.

Rowe, M. D, C. W. Fairall, and J. A. Perlinger (2011), Chemical sensor resolution requirements for near-surface measurements of turbulent fluxes, *Atmos. Chem. Phys.*, *11*, 5263–5275.

Singh, H. B., M. Kanakidou, P. J. Crutzen, and D. J. Jacob (1995), High concentrations and photochemical fate of oxygenated hydrocarbons in the global troposphere, *Nature*, *378*, 50–54.

Singh, H. B., A. Tabazadeh, M. J. Evans, B. D. Field, D. J. Jacob, G. Sachse, J. H. Crawford, R. Shetter, and W. H. Brune (2003), Oxygenated volatile organic chemicals in the oceans: Inferences and implications based on atmospheric observations and air-sea exchange models, *Geophys. Res. Lett.*, *30*(16), 1862, doi:10.1029/2003GL017933.

Singh, H. B., et al. (2004), Analysis of the atmospheric distribution, sources and sinks of oxygenated volatile organic chemicals based on measurements over the Pacific during TRACE-P, *J. Geophys. Res.*, *109*, D15S07, doi:10.1029/2003JD003883.

Sinha, V., J. Williams1, M. Meyerhöfer, U. Riebesell, A. I. Paulino, and A. Larsen (2007), Air-sea fluxes of methanol, acetone, acetaldehyde, isoprene and DMS from a Norwegian fjord following a phytoplankton bloom in a mesocosm experiment, *Atmos. Chem. Phys.*, *7*, 739–755.

Sjostedt, S. J, W. R. Leaitch, M. Levasseur, M. Scarratt, S. Michaud, J. Motard-Côte, J. H. Burkhart, and J. P. D. Abbatt (2012), Evidence for the uptake of atmospheric acetone and methanol by the Arctic Ocean during late summer DMS-Emission plumes, *J. Geophys. Res.*, *117*, D12303, doi:10.1029/2011JD017086.

Staudt, A. C., D. J. Jacob, F. Ravetta, J. A. Logan, D. Bachiochi, T. N. Krishnamurti, S. Sandholm, B. Ridley, H. B. Singh, and B. Talbot, (2003), Sources and chemistry of nitrogen oxides over the tropical Pacific, *J. Geophys. Res.*, *108*(D2), 8239, doi:10.1029/2002JD002139.

Taddei, S., P. Toscano, B. Gioli, A. Matese, F. Miglietta, F. P. Vaccari, A. Zaldei, T. Custer, and J. Williams, Carbon dioxide and acetone air-sea fluxes over the Southern Atlantic, *Environ. Sci. Technol.*, *43*, 5218–5222.

Takahashi, T., et al. (2009), Climatological mean and decadal change in surface ocean pCO_2 and net sea-air CO_2 flux over the global oceans, *Deep Sea Res., Part II*, *56*, 554–577.

Tarran, G. A., J. L. Heywood, and M. V. Zubkov (2006), Latitudinal changes in the standing stocks of nano- and picoeukaryotic phytoplankton in the Atlantic Ocean, *Deep Sea Res., Part II*, *53*, 1516–1529.

Tie, X., A. Guenther, and E. Holland (2003), Biogenic methanol and its impacts on tropospheric oxidants, *Geophys. Res. Lett.*, *30*(17), 1881, doi:10.1029/2003GL017167.

Tilstone, G. H., T. J. Smyth, A. J. Poulton, and R. Hutson (2009), Measured and remotely sensed estimates of primary production in the Atlantic Ocean from 1998 to 2005, *Deep Sea Res., Part II*, *56*, 918–930.

Williams, J., R. Holzinger, V. Gros, X. Xu, E. Atlas, and D. W. R. Wallace (2004), Measurements of organic species in air and seawater from the tropical Atlantic, *Geophys. Res. Lett.*, *31*, L23S06, doi:10.1029/2004GL020012.

Zhou, X., and K. Mopper (1997), Photochemical production of low-molecular-weight carbonyl compounds in seawater and surface microlayer and their air-sea exchange, *Mar. Chem.*, *56*, 201–213.